IOP Publishing | Astro Ltd Laser Physics

Laser Phys. **28** (2018) 025701 (5pp) https://doi.org/10.1088/1555-6611/aa92f6

YAG:Yb^{3+} crystal as a potential material for optical temperature sensors

H G Demirkhanyan[1], G G Demirkhanyan[1,2] and R B Kostanyan[2]

[1] Armenian State Pedagogical University after Kh. Abovyan, Yerevan, Armenia
[2] Institute for Physical Research of NAS of Armenia, Ashtarak, Armenia

E-mail: demirkhanyan.hasmik@aspu.am

Received 24 April 2017, revised 24 September 2017
Accepted for publication 10 October 2017
Published 22 January 2018

Abstract

The possibilities are discussed of $Y_3Al_5O_{12}$:Yb^{3+} crystal as a material for an optical temperature sensor (OTS) based on the temperature dependences of the more intense spectral emission lines and on the ratio of the absorption coefficients from the ground and first excited Stark sublevels. The operating temperature and average sensitivity for OTSs are determined. It is shown that the former is an effective method for an OTS in a cryogenic temperature range (40–130 K) and the latter in a high temperature range (500–1000 K).

Keywords: optical temperature sensor, rare earth ions, zero-phonon line intensity

(Some figures may appear in colour only in the online journal)

1. Introduction

Optical sensors are sensitive devices based on detecting variations in intensity (or in phase) of one or more light beams that interact with physical systems. Intensive research into the possibilities for new optical sensors is motivated by their clear advantages such as high sensitivity and a wide range of areas of application (chemical and biochemical changes, measurement of deformations, temperature, pressure etc).

Optical temperature sensors (OTS) are a special case among optical sensors. They can be effectively used for measurement and control of temperature in cases where conventional techniques cannot be used and/or have significant drawbacks. Optical temperature sensors have significant advantages over conventional ones in electrical passivity, greater sensitivity, protection from electromagnetic noise and wide dynamic range. To send and receive optical signals over long distances a network of sensors or sensor arrays are used. When using optical sensors in such situations it is not necessary to make a conversion between electronics and photonics at each sensing point, thereby increasing overall flexibility and reducing costs. Among the possible applications of OTSs are monitoring temperature in highly corrosive media, electrical power stations, oil refineries, coal mines and fire detection systems.

Materials doped with rare earth (RE^{3+}) ions are known for temperature-dependent spectroscopic characteristics (fluorescence intensities, fluorescence lifetimes, absorption coefficients etc) in the infrared and visible range. This makes them good candidates for optical sensors in general and OTSs in particular. But, as a rule, their use in OTSs based on fluorescence intensity ratio (FIR) is limited, assuming that the temperature dependence of the FIR is conditioned by the Boltzmann factor of the population of neighboring energy levels [1–6]. In [7–9] an average time of fluorescence (FL) from two nearby levels is considered as a temperature-dependent measured value (figure 1(a)). Here, it is assumed that the time required for thermalization between two excited levels i and j is shorter than their spontaneous lifetimes $\tau_i = A_{i0}^{-1}$ and $\tau_j = A_{j0}^{-1}$. Note that during the search for new materials and mechanisms for temperature sensing it is necessary to consider that thermally coupled operating energy levels of an OTS must satisfy the following conditions.

1. The energy gap between initial levels
   - must be at least $\sim 200\,\mathrm{cm}^{-1}$, which will guarantee the required solvability of the corresponding spectral lines,
   - must not exceed $\sim 2000\,\mathrm{cm}^{-1}$ to ensure the required population of the initial levels in a given temperature range.
2. The energy gap between the initial level and the nearest lower level should be large enough (more than six times larger than the Debye phonon energy of the considered

 © 2018 Astro Ltd Printed in the UK

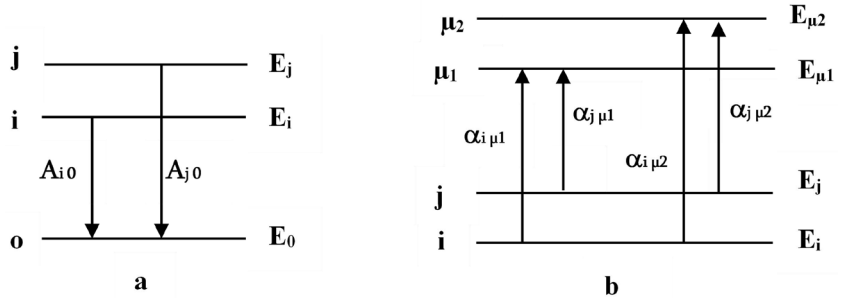

Figure 1. Schemes for OTSs operated on (a) FIR and (b) ACR methods.

material). This will guarantee domination of radiative transitions over non-radiative ones.

So far, a large number of distributed and point OTSs based on glasses, ceramics and fibers doped with different RE^{3+} ions (Er^{3+}, Sm^{3+}, Eu^{3+}, Pr^{3+}) have been presented [1–3, 10]. OTSs based on these materials have the ability to cover a wide temperature range (300 to 1623 K) with reasonable measurement resolution [3–6]. However, not much research work has been carried out on Yb^{3+}-doped materials for such purposes. As a rule, the ytterbium ion is used as a co-activator to enhance the efficiency of the up-conversion luminescence of erbium, holmium, thulium ions, etc [11–13]. In particular, Kennedy and Djeu have reported fiber-optic temperature sensors based on fluorescence decay in Yb^{3+}-doped yttrium aluminum garnet (YAG) and YAG:Yb^{3+},Tb^{3+} [12]. Wade *et al* [14] have reported the FIR-based temperature sensing performance of Yb^{3+}-doped silica fiber using Stark sublevels of the $^2F_{5/2}$ state of the Yb^{3+} ion. The possibilities of using Yb^{3+}-doped $NaBi(WO_4)_2$ and $LiNbO_3$ crystals as materials for OTS have been reported in [15].

In this paper the possibilities of Yb^{3+}-doped YAG crystal as a material for an OTS based on absorption coefficient ratio (ACR) as well on zero-phonon line intensity (ZPLI) of fluorescence are discussed.

2. ACR method

The scheme of the ACR method is given in figure 1(b). Here the ratio of absorption coefficients from two Stark sublevels i and j of the ground manifold is used as a temperature-dependent measure. The final state of transitions may be either one level or two different levels, depending on the line strengths of the corresponding transitions (figure 1(b)). It is known that the shift in energy levels in RE^{3+}-doped crystals during electron transitions is less than the widths of the corresponding spectral lines, so the ratio of absorption coefficients from the ground and first excited states (transitions $i \to \mu_p$ and $j \to \mu_k$) may be approximately represented by

$$R_{\text{abs}} = \frac{\alpha_{j\mu_k}}{\alpha_{i\mu_p}} = D \exp\left(\frac{-\Delta E_{ji}}{kT}\right), \tag{1}$$

where D is determined by the expression

$$D = \frac{n_{i\mu_p}^2 \lambda_{i\mu_p} \Gamma_{i\mu_p} S_{j\mu_k}}{n_{j\mu_k}^2 \lambda_{j\mu_k} \Gamma_{j\mu_k} S_{i\mu_p}}. \tag{2}$$

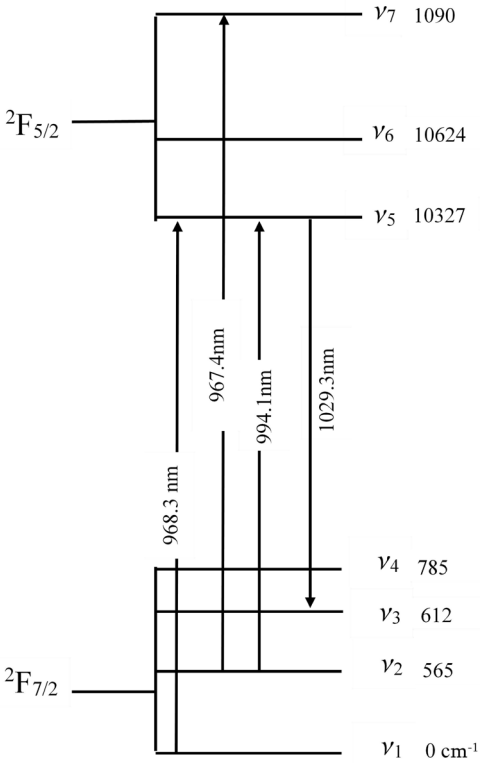

Figure 2. Energy scheme of Stark sublevels of YAG:Yb^{3+} crystal.

$\Gamma_{i\mu}$ and $S_{i\mu}$ are correspondingly the width and line strengths of the transition $i \to \mu$, ΔE_{ji} is the energy gap between initial levels, n_{ij} is the refractive index at the transition wavelength, k is Boltzmann's coefficient and T is temperature. It can be seen that, in general, besides the Boltzmann factor, the temperature dependence of R_{abs} has a certain contribution from the homogeneous widths of the corresponding spectral lines. However, the ratio $\frac{\Gamma_{i\mu_p}}{\Gamma_{j\mu_k}}$ is weak compared to the Boltzmann factor, and, as a rule, it can be neglected. Finally, assuming that the temperature dependence of R_{abs} is fully determined by the Boltzmann factor, the sensitivity of the ACR method, determined by the expression $S_{\text{R}}(T) = \frac{1}{R}\frac{\text{d}R}{\text{d}T}$, will be

$$S_{\text{R}}(T) = \frac{\Delta E_{ji}}{kT^2}. \tag{3}$$

Note that since sensitivity itself depends on temperature, it is convenient to determine the average sensitivity as an OTS characteristic from the expression

Table 1. Spectroscopic characteristics of YAG: Yb^{3+} crystals.

Transition	$\nu_1 \rightarrow \nu_5$	$\nu_2 \rightarrow \nu_7$	$\nu_2 \rightarrow \nu_6$	$\nu_5 \rightarrow \nu_3$	References
Wavelength (nm)	968.3	967.4	994.1	1029.3	[10]
Line strength (10^{-20} cm^2)	0.1016	0.0717	0.1711	0.1878	[11]
Width of ZPL (cm^{-1})					
500–1000 K	10.7–27.2	54.0–95.8	43.9–87.2	16.3–39.8	[14]
77–300 K	0.1–4.6	25.6–38.2	14.9–27.6	0.2–7.2	
Debye–Waller factor					
at 500–1000 K	0.03–0.06	0.44–0.84	2.12–4.05	13.68–26.19	[14]
at 77–300 K	0.01–0.02	0.17–0.29	0.80–1.39	5.17–9.0	

$$\overline{S}_{\mathrm{R}} = \frac{1}{\Delta T}\int_{T_1}^{T_2} S\,(T)\ \mathrm{d}T. \tag{4}$$

In particular, for the ACT method, taking into account (3), we will obtain

$$\overline{S}_{\mathrm{R}}^{(\mathrm{ACR})} = \frac{\Delta E_{ji}}{kT_1T_2}, \tag{5}$$

where $\Delta T = T_2 - T_1$ is the width of the operational temperature range.

3. ZPLI method

This method is based on the temperature dependence of the ZPLI, which is induced by inter-Stark transitions. It is well known that the temperature dependence of the ZPLI is defined by temperature dependences of homogeneous width $\Gamma(T)$, shift $\Delta\varepsilon(T)$ and Debye–Waller (D–W) factor $2M(T)$ of the spectral line. The intensity of a zero-phonon line having a Lorentzian contour can be represented by the expression

$$I(T) = C \times \frac{\Gamma(T)}{[\Delta\varepsilon(T)]^2 + \Gamma^2(T)}\exp[-2M(T)], \tag{6}$$

where C is a temperature-independent value. As a temperature-dependent value, the relative intensity of the most intense zero-phonon spectral line is considered:

$$R = \frac{I(T)}{I(T_0)} = B \times \frac{\Gamma(T)}{[\Delta\varepsilon(T)]^2 + \Gamma^2(T)}\exp[-2\,M(T)], \tag{7}$$

where $B = \frac{[\Delta\varepsilon(T_0)]^2+\Gamma^2(T_0)}{\Gamma(T_0)}\exp[2M(T_0)]$ is calculated at fixed temperature T_0. Then for the sensitivity of the ZPLI method we obtain

$$S = 2\frac{\mathrm{d}M}{\mathrm{d}T} + \frac{1}{\Gamma}\frac{\mathrm{d}\Gamma}{\mathrm{d}T} + \frac{2(\Delta\varepsilon)^2}{(\Delta\varepsilon)^2 + \Gamma^2} \times \left(\frac{1}{\Delta\varepsilon}\frac{\mathrm{d}\Delta\varepsilon}{\mathrm{d}T} - \frac{1}{\Gamma}\frac{\mathrm{d}\Gamma}{\mathrm{d}t}\right). \tag{8}$$

In particular, for RE^{3+}-doped bulk single crystals the temperature shifts of levels are insignificant ($\Delta\varepsilon \approx 0$) for purely electronic transitions. Thus by neglecting the third term in (8), we will obtain the expressions for sensitivity,

$$S = 2\frac{\mathrm{d}M(T)}{\mathrm{d}T} + \frac{\mathrm{d}\ln\Gamma(T)}{\mathrm{d}T}, \tag{9}$$

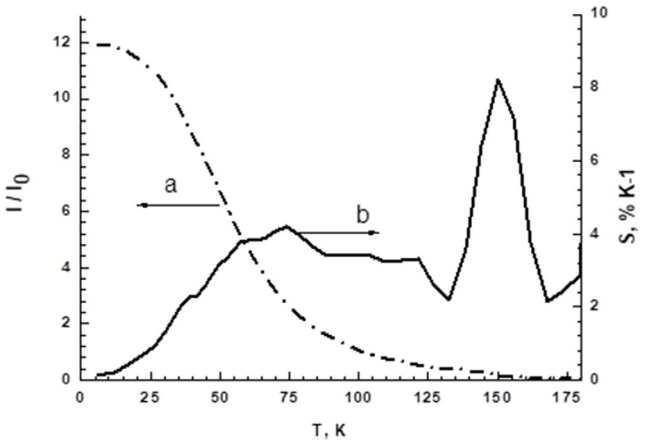

Figure 3. Temperature dependence of (a) the relative intensity of fluorescence at a wavelength of 1029.3 nm and (b) the sensitivity of the OTS from the ZPLI method for YAG:Yb^{3+} crystal.

and for average sensitivity in the temperature range $T_1 \leqslant T \leqslant T_2$,

$$\overline{S} = 2\Delta M + \ln\frac{\Gamma(T_2)}{\Gamma(T_1)}, \tag{10}$$

where $\Delta M = M(T_2) - M(T_1)$. As is seen from (10), the main contribution to the value of $\overline{S}$ is determined by the increment of the D–W factor in the operating temperature range.

4. The sensing properties of YAG:Yb^{3+} crystal

It is well known that the energy scheme of the ground electronic configuration ($4f^{13}$) of the Yb^{3+} ion has only two manifold groups: $^2F_{7/2}$ and $^2F_{5/2}$ (figure 2). Therefore, for studying spectroscopic properties of Yb^{3+}-doped crystals, it is necessary to take into account the Stark structure of the optical spectrum of the impurity ion.

The spectroscopic and kinetic characteristics of the YAG:Yb^{3+} crystal are thoroughly investigated in [16–18]. In particular, line strengths of inter-Stark transitions are calculated in [18], and the main spectroscopic characteristics (absorption coefficients, probabilities of spontaneous transitions etc) are determined based on those. Experimental and theoretical studies of the temperature dependences of ZPLI of fluorescence in the wavelength range 960–1030 nm are given in [19, 20]. The values of the spectroscopic characteristics required for subsequent quantitative estimates of the sensing

Table 2. Operating properties of the OTS.

	YAG:Yb^{3+}		BiLiBaPb:Er^{3+} [23]	SiO_2:Sm^{3+} [21]
Characteristics of OTS	ZPLI	ACR	FIR	FIR
Operating temperature range (K)	40–130	500–1000	296–603	295–748
Sensitivity at T_0 (K)	40	500	296	296
Sensitivity at T_0 (% K^{-1})	2.2	0.31	0.44	1.84
Average sensitivity (% K^{-1})	3.4	0.16	—	—

characteristics of YAG:Yb^{3+} crystal on the basis of the ZPLI and ACR methods are given in table 1.

4.1. YAG:Yb^{3+} sensors in the ZPLI method

It is shown in [19, 20] that the intensity of fluorescence at a wavelength of 1029.3 nm increases sharply when the temperature drops below that of liquid nitrogen. This suggests that the YAG:Yb^{3+} crystal is a promising material for ZPLI-based OTSs in the cryogenic temperature range.

Hereafter, the intensity of impurity radiation at 1029.3 nm is taken as a temperature-dependent value. We can determine the temperature dependence of the relative intensity $\frac{I(T)}{I(T_0)}$ of fluorescence at this wavelength, as well as the value of the parameter $B(\lambda)$ in (7): $B(1029.3) = 7.24\,\mathrm{cm}^{-1}$ using the temperature dependences of the spectral characteristics of zero-phonon lines (homogeneous widths, shifts and D–W factors) found in [20]. Figure 3 shows the temperature dependences of relative intensity $\frac{I(T)}{I(T_0)}$ ($T_0 = 77\,\mathrm{K}$) and sensitivity determined by (9). It is seen that when the temperature is lowered from 100 K to 10 K, the radiation intensity increases by a factor of 12, which provides a high sensor sensitivity of the ZPLI method for YAG:Yb^{3+}. At the same time, in the temperature range 30–77 K, the dependence of the relative intensity on temperature is nearly linear. The values of the main characteristics of the OTS based on this method are given in table 2.

4.2. YAG:Yb^{3+} sensors in the ACR method

From the energy-level scheme of the Yb^{3+} ion in YAG it is seen that the first excited Stark level ν_2 is separated from the ground level ν_1 by an energy gap of $565\,\mathrm{cm}^{-1}$ (figure 2). Thus, the ACR method can be effective at sufficiently high temperatures ($T \geqslant 500\,\mathrm{K}$), providing the necessary population ($\sim 20\%$) of the ν_2 excited level.

For this crystal the ratio of the absorption coefficients can be considered as a temperature-dependent value at wavelengths of 994.1 nm and 968.3 nm, which are caused by transitions $\nu_2 \to \nu_6$, $\nu_1 \to \nu_5$ and $\nu_2 \to \nu_7$ (figure 2). Then

$$R_{\mathrm{abs}} = \frac{\alpha_{\nu_2\to\nu_6}}{\alpha_{\nu_1\to\nu_5} + \alpha_{\nu_2\to\nu_7}} = \frac{D\exp\left(\frac{-\Delta E}{kT}\right)}{1 + D_1\exp\left(\frac{-\Delta E}{kT}\right)}, \quad (11)$$

where $\Delta E = \varepsilon_2 - \varepsilon_1 = 565\,\mathrm{cm}^{-1}$, coefficients D and D_1 are defined by (2) and for the transitions $\nu_2 \to \nu_6$, $\nu_1 \to \nu_5$ and $\nu_2 \to \nu_7$:

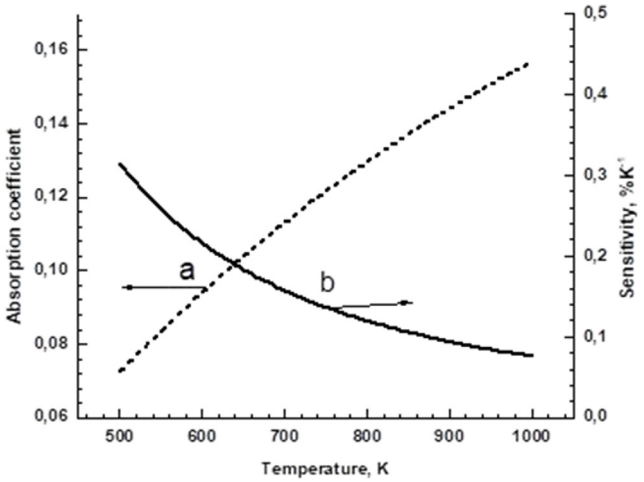

Figure 4. Temperature dependence of (a) ACR at wavelengths of 994.1 and 968.3 nm and (b) the sensitivity of the OTS from the ACR method for YAG:Yb^{3+} crystal.

$$D = \frac{\lambda_{\nu_1\to\nu_5}\Gamma_{\nu_1\to\nu_5}\,S_{\nu_2\to\nu_6}}{\lambda_{\nu_2\to\nu_6}\Gamma_{\nu_2\to\nu_6}\,S_{\nu_1\to\nu_5}} \quad \text{and} \quad D_1 = \frac{\Gamma_{\nu_1\to\nu_5}\,S_{\nu_2\to\nu_7}}{\Gamma_{\nu_2\to\nu_7}\,S_{\nu_1\to\nu_5}}. \quad (12)$$

In (12) we assumed that the value of the refractive index in the considered wavelength range is constant and within the widths of the considered zero-phonon lines: $\lambda_{\nu_1\to\nu_5} \approx \lambda_{\nu_2\to\nu_7} \approx 968.3\,\mathrm{nm}$. Then the temperature dependence of sensitivity can be presented in the form

$$S(T) = \frac{1}{1 + D_1\exp\left(\frac{-\Delta E}{kT}\right)} \times \frac{\Delta E}{kT^2}, \quad (13)$$

and the average sensitivity in the temperature range $[T_1,\ T_2]$ as

$$\overline{S} = \ln\frac{D_1 + \exp\left(\frac{\Delta E}{kT_1}\right)}{D_1 + \exp\left(\frac{\Delta E}{kT_2}\right)}. \quad (14)$$

Values of the coefficients D and D_1 will be determined using values of spectroscopic characteristics calculated from the formulas of [18, 20] (table 1). Numerical estimates show that in the temperature range 500–1000 K ratios of homogeneous widths vary within $0.2 \leqslant \frac{\Gamma(968)}{\Gamma(994)} \leqslant 0.24$ and $0.2 \leqslant \frac{\Gamma(968)}{\Gamma(967)} \leqslant 0.28$. For numerical estimates, we used $\frac{\Gamma_{\nu_1\to\nu_5}}{\Gamma_{\nu_2\to\nu_6}} \approx 0.22$ and $\frac{\Gamma_{\nu_1\to\nu_5}}{\Gamma_{\nu_2\to\nu_7}} \approx 0.24$. Thus, according to (12) and by using the data of table 1, we obtained the values

0.38 and 0.17 for the coefficients D and D_1, respectively. The temperature dependences of the ACR $R_{abs}(T)$ and the sensitivity $S(T)$ are given in figure 4.

It is seen that in the temperature range 500–1000 K the ACR smoothly, almost linearly, changes by a factor of two, which makes it possible to register temperature in steps of 50 K at an average sensitivity of $\overline{S} = 0.16\%\,\mathrm{K}^{-1}$.

5. Summary

In the cryogenic temperature range, the YAG:Yb^{3+} crystal has revealed excellent sensing capabilities based on the ZPLI method. This is noteworthy because already known OTSs based on RE^{3+}-doped materials, which operate on the FIR method, are effective at higher temperature (room temperature and above). At the same time, the average sensitivity of an OTS based on YAG:Yb^{3+} crystal, operating on the ZPLI method, is $3.4\%\,\mathrm{K}^{-1}$ in the temperature range 40–130 K, which is an order of magnitude larger than the sensitivity of a resistive temperature sensor ($0.3\%\ \mathrm{K}^{-1}$) [22]. On the other hand, the YAG:Yb^{3+}-based OTS from the ACR method effectively operates in a high temperature range (500–1000 K) and its sensitivity is comparable to that of other sensors [23].

References

[1] Rai K V 2007 *Appl. Phys.* B **88** 207
[2] Rai K V 2007 *Appl. Phys.* B **87** 323
[3] Rai V K, Rai D K and Rai S B 2006 *Sensors Actuators* A **128** 14
[4] Camargo A S *et al* 2006 *Solid State Commun.* **137** 1
[5] Feng L, Lai B, Wang J and Dua G Su Q 2010 *J. Lumin.* **130** 2418
[6] Li C, Dong B, Li Sh and Song Ch 2007 *Chem. Phys. Lett.* **443** 426
[7] Zhang Z Y, Sun T, Grattan K T V and Palmer A W 1998 *Sensors Actuators* A **71** 183
[8] Sun T, Zhang Z Y, Grattan K T V and Palmer A W 1998 *Rev. Sci. Instrum.* **69** 4179
[9] Rai N and Rai V K 2007 *Sensors Transducers J.* **77** 1040
[10] Pandey A and Rai V K 2014 Rare earth doped materials for temperature sensors *Spectroscopic Techniques for Security Forensic and Environmental Applications* ed Y Dwivedi *et al* (New York: Nova) ch 11 pp 279–92
[11] Liu G, Fu L, Gao Zh, Yang X, Fu Z, Wang Zh and Yang Y 2015 *RSC Adv.* **5** 51820
[12] Kennedy J L and Djeu N 2002 *Sensors Actuators* A **100** 187
[13] Rakov N and Maciel G 2017 *J. Appl. Phys.* **121** 113103
[14] Wade S A, Collins S F and Baxter G W 2003 *Appl. Phys.* **94** 4743
[15] Demirkhanyan H, Demirkhanyan G, Kokanyan E, Kostanyan R and Aillerie M 2012 *Proc. SPIE* **8414** 84140Q
[16] Krupke W F 2000 *IEEE J. Sel. Top. Quantum Electron.* **6** 1287
[17] DeLoach L D, Payne S A, Chase L L, Smith L K, Kway W L and Krupke W F 1993 *IEEE J. Quantum Electron.* **29** 1179
[18] Demirkhanyan G G 2006 *Laser Phys.* **16** 1054
[19] Kawanaka J *et al* 2005 *Laser Phys.* **15** 1306
[20] Demirkhanyan G G and Kostanyan R B 2008 *Laser Phys.* **18** 104
[21] Alves R B, Christol J, Sun M and Wickersheim K A 1983 *Proc. ISA Int. Conf. and Exhib. (Houston, TX)* p. 925
[22] Tripathi G, Rai V K and Rai S B 2007 *Opt. Mater.* **30** 201
[23] Jung J and Lee B 1999 *Proc. SPIE* **3746** 538